Available online at www.sciencedirect.com
ScienceDirect
Materials and Design 29 (2008) 839–851
Materials & Design
www.elsevier.com/locate/matdes

Capacitor discharge welded bars of Inconel 718 and TiAl6V4 superalloys under fatigue

S. Chiozzi *, V. Dattoma, F. Panella

Department of "Ingegneria dell'Innovazione", University of Lecce, I-73100 Lecce, Italy

Received 7 December 2006; accepted 14 March 2007
Available online 27 March 2007

Abstract

This work concerns the mechanical behaviour analysis of Capacitor Discharge Welded joints made with Inconel 718 and TiAl6V4 superalloys in the form of cylindrical bars. The research activities have been conducted in the frame of AWFORS project, financed by the European Community. The Capacitor Discharge Welding (CDW) technique is of particular interest for repair processes; it allows the substitution of the damaged part after its removal and the replacement of the new component without consistent additional machining. Good mechanical properties and geometrical integrity are to be achieved; consequently, the multipoint contact profile for the CDW process has been conceived to enhance the microstructural weld characteristics and improve the fatigue and creep behaviour at high temperatures.

Fatigue tests have been performed both at room and working temperature, comparing the results between base material and as-welded specimens with the same heat treatment. The microstructure has been deeply analyzed through optic and scanning electron microscope (SEM) observations; this way the microstructural modifications and the Heat Affected Zones have been studied in the welded section as well as the interaction between the weld layers material and the parent metal.

Keywords: Welding (D); Fatigue (E); Creep (I)

1. Introduction

In this work, the mechanical characterization of CD Welded bars made with Inconel 718 and Titanium TiAl6V4 superalloys is presented, completed with microstructural and fracture analyses. These materials are currently used in the aeronautical field for fabrication purposes of turbine blades and special parts; the static and fatigue properties at room and working temperature of the welded joints have to be investigated, since the development of advanced technologies for the repair of aeronautical components is of particular interest in the recent years. The Capacitor Discharge Welding (CDW) technology allows the removal of the damaged part and the subsequent substitution of a the new component without the replacement of the whole block and additional machining. In addition, good mechanical and geometrical integrity properties are to be achieved with the aid of a specially conceived multipoint welding profile for the CDW process. Aeronautical industries are interested into this welding technology and the University of Lecce has an active role in the process development and in the mechanical improvements, as well as the microstructural characterisation of the welded pieces is considered. Demands for improved aeronautical repair methods with new blade concepts (e.g. Blade Integrated Disks – BLISKs) are also required with the new available welding technologies to be applied for compressor BLISKs and High Pressure Turbine (HPT) blades; BLISKs are disks with integrated blading, 30% lighter than conventional disks, but the damage occurrence even on the single blade is critical for operating reliability after the blade replacement with the new procedures.

* Corresponding author. Tel.: +39 832297776; fax: +39 832297279.
E-mail address: samanta.chiozzi@unile.it (S. Chiozzi).

0261-3069/$ - see front matter © 2007 Elsevier Ltd. All rights reserved.
doi:10.1016/j.matdes.2007.03.011

Repair methods usually employed, such as TIG welding and laser cladding, lead to large heat-affected zones (HAZ) and elevated distortion is induced in the component; these technologies are well suitable for small parts repairs and blade tip reconstruction. As an alternative to the above-stated methods, linear friction welding and laser welding may also produce too large deformations and the process applicability is problematic due to the complex geometries to be welded in the case of blade-to-rotor joints. Capacitor Discharge Welding (CDW) provides drastic reductions in the size of the weld cord and HAZ, assures good mechanical properties and the required service life of the welded parts, with an higher level of dimensional accuracy and elevated process automation ability [4–7]. At present time the CDW process for aeronautical repairs is under analysis because of the lack of enough experimental data on this technology as function of the welding parameters, especially in the case of advanced materials applications.

The CDW technology is to be implemented and verified under oscillating loads and creep, in order to ensure the welding quality and the process feasibility according to the technological parameters and the joint geometry; in fact, the welded section microscopic and SEM observation showed diversified distribution of the welded metal in extremely thin layers between the welded parts in the order of 0.1 mm and extremely fine grain size zones at the transition interface with high precipitates density. Tensile, creep and fatigue tests have been performed both at room and working temperature comparing the results between base material and as-welded specimens with the same heat treatments. This way the CDW process applied on cylindrical bars with the multipoint profile geometry has been deeply analyzed on aeronautical materials in terms of structural capabilities and microstuctural properties for the development of this promising technology.

2. CDW technology applications

The CD Welding process is a pulsed power application which makes use of a large electrical capacity stored in a capacitor battery; it is actually used to rapidly weld small dices and pins onto metallic structures and is currently available for new applications through special CDW electrical machines. The CD Welding cycle is based on four successive phases (Fig. 1a); initially the surfaces of the two parts to be welded are connected with the machine electrodes and positioned oppositely each other by means of special gripping tools. In the second phase, the parts are put in contact through a special igniter to be machined on one of the two opposite surfaces and a calibrated compressive force is applied; successively, the stored input energy is released in the third phase with secondary transformer circuits (Fig. 1b) and the electrical discharge takes place in the welding spot; the current is in the order of 100 kA and provokes the instantaneous evaporation or fusion of the igniter in a time interval of about 10 ms; this way the welding spot is heated and the surfaces are melted

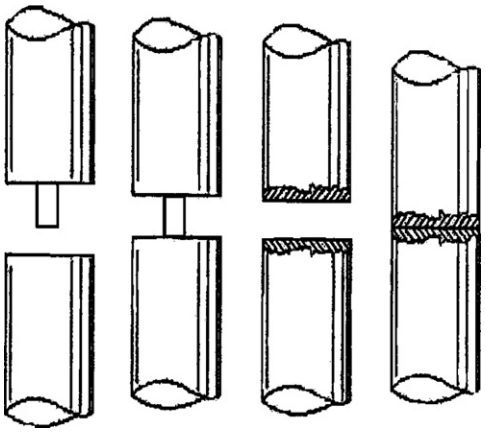

Fig. 1a. The CDW process phases.

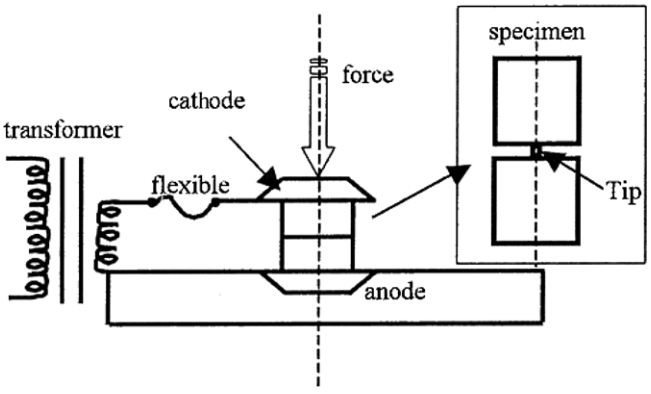

Fig. 1b. CD Welding electrical discharge.

and joined once the igniter is collapsed. In the final phase a forging force is still applied, the liquefied metal solidifies and the welding junction occurs with a thin welded layer between the parts.

The CDW process offers the following characteristics:

- limited deformations are produced in the welded components outside the welding area and less material is expulsed from the welded zone;
- stress concentration effects are avoided at the weld toe and good material continuity is reached;
- minimum extension of the Heat Affected Zone and extremely thin welded material are achieved;
- uniform and rapidly solidified material distribution with fine grain dimensions; cracks and porosity are totally absent if the correct technological parameters are determined.

The CDW process is controlled mainly by the modification of the technological parameters (input energy, applied pressure and electrical circuit setup) and through accurate design of the welding section geometry and igniter volumes; the maximum current flux can be measured and the extension of the effective welded area can be extended also by means of special electrodes shape and gripping fea-

tures, in order to reduce the conductivity losses and to assure good alignment and elevated welding pressures.

A special welding tool has been designed in order to clamp the selected circular specimens into the capacitor welding machine (Fig. 2a) and to correctly apply the needed pressures and energy with the aid of flexible conical grips (Fig. 2b) to be mounted beside the specimens in the maximal proximity of the welding spot. The electrical resistances of the welding circuit of which the specimens and the electrodes belong to and the contact losses are consequently reduced and an area of approximately 130 mm^2 (according to a bore diameter of 12 mm for the Inconel 718 and TiAl6V4 bars) is possible to be welded also for materials with high temperature capabilities; up to now in fact, the technical literature says only small components with 6 mm diameters made of simple steel have been successfully welded with the CDW technique. More over, the parts mutual slipping during welding, concentricity defects and contact dispersions are avoided: the electrical current flux reaches the parts to be welded through pure copper made components and grips, while pressure is applied by the upper steel plate, between the lateral sliding guides.

Each part of the specimen is positioned into the copper cylindrical supports of Fig. 2b; the flexible grips and the concentricity between the parts are set through a screwing system between the conical grips and the internally threaded cylinders.

After preliminary CD Welding campaigns on steel bars with different materials [1,3] and preliminary numerical studies of the electrical discharge phenomena [2,10,13], the single igniter technique has been abandoned and replaced with a new contact geometrical profile (Fig. 3), conceived to enhance the process applicability on larger components with advanced materials; the special welding profile is a multipoint linear contact profile to be machined on one or both the surfaces to be welded with special grinding tools with small radius [8,9]. It has been studied with narrow gaps alternated to contact peaks in the form of two coupled sinusoidal profiles, in order to allow the CDW process to fully take place and improve the welding characteristics; the parts are put in contact through multipoint igniting zones and the discharged energy is better distributed all over the welding section. The welded surface extension is limited for conventional CDW technology by the current discharge curve shape, inductive phenomena and maximum power input; thereafter the choice of several

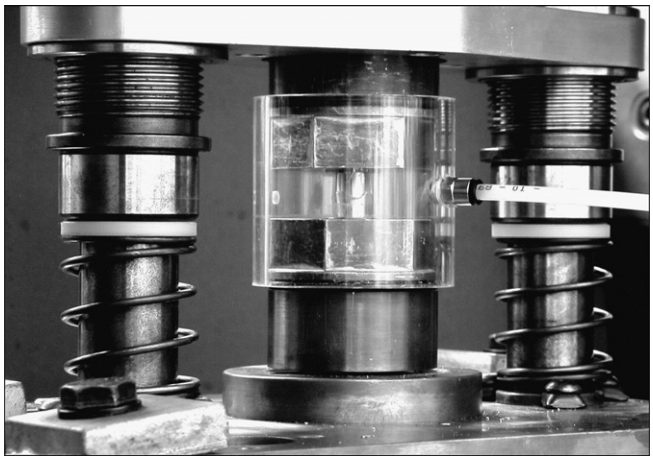

Fig. 2a. The CDW process tool with gas shielding.

Fig. 2b. Flexible grips for CDW.

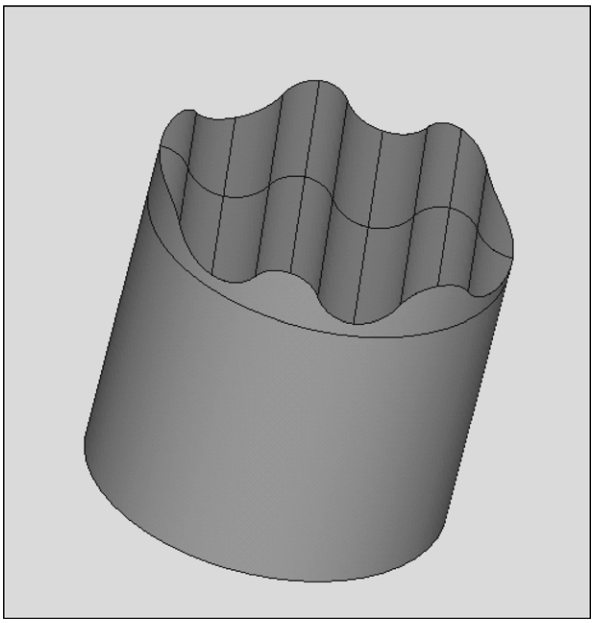

Fig. 3a. The multipoint CDW profile.

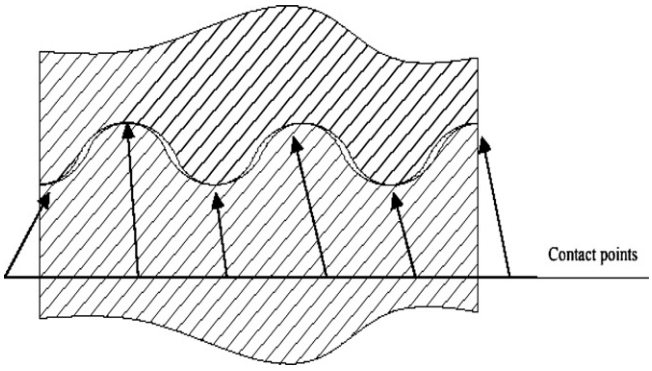

Fig. 3b. Welding cylindrical parts in contact.

igniting peaks, alternated with calibrated gaps of only 0.4 mm depth. The welding process is localized in parallel regions of smaller width. The sinusoidal shape is needed to avoid geometrical discontinuities between the contact regions and the open gaps; this way the molten material flows from the contact peaks to fill the remaining voids in the welded section and allows to control the total deformation of the welded joint and to avoid the geometrical collapse. In addition, the vain design optimizes the outlet flow for the forging material; simultaneously, the constant presence of calibrated pressure allows the joint in perfect welding conditions and will facilitate the expulsion of the entrapped gas developed during the electric discharge.

With the proposed contact profile applied to the aeronautical alloys, it has been possible to perform the CDW butt joints only by using multiple discharges, since elevated temperatures had necessarily to be achieved in the welding zone; the first discharge is aimed to pre-heat the specimen and the last one will produces the melting and forging phase for the weld to occur. The weld is progressively extended due to elevated pressures applied between the electrodes and the Joule effect at each contact peaks. At the same time, the local resistivity increase with higher temperatures allows the full jointed bars to be successfully welded.

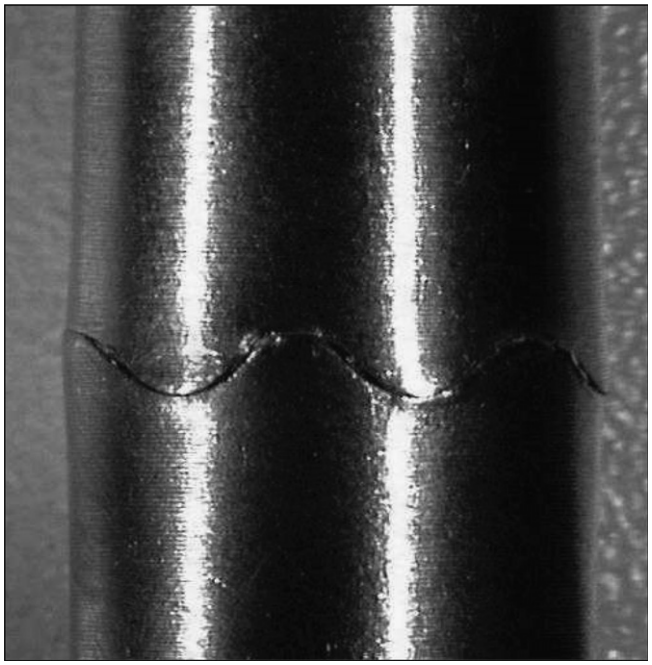

Fig. 4a. Partially welded specimen.

Table 1
Optimal welding parameters ranges (exact values are here omitted)

Material type	No. of discharges	Energy input (kJ)	Applied force (kN)	Maximum current (kA)
Inconel 718	3	30–50	30–60	~90
TiAl6V4	2	20–40	20–50	~60

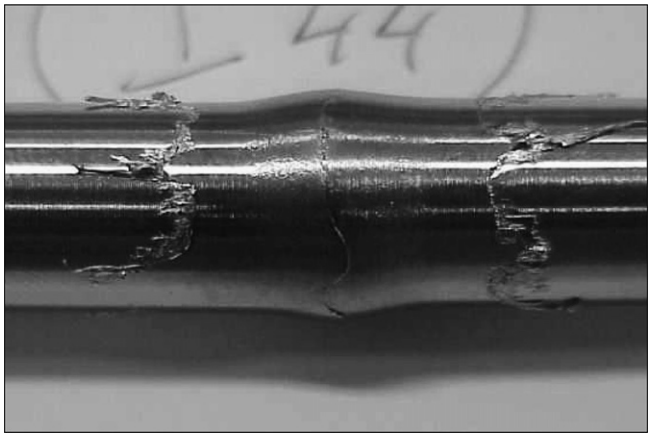

Fig. 4b. Welded specimen for Ti bars with the multipoint technique.

Different welding parameters combinations have been considered with multiple discharges in a number of 2–5; this way some specimens did not successfully weld (Fig. 4a), with the consequent separation of the two edges or burnout of the welded profile; finally, the parameters have been optimized in Table 1 and 40 specimens have been welded with good results for both the materials. The base metal bars have been welded in the ''annealed'' conditions for Ti alloy and ''Solution-precipitated'' conditions for Inconel 718, following the AMS specified thermal conditions and post-welding heat treatments are also needed. Gas shielding has been applied with pure Argon inflated in a special chamber around the welding spot (Fig. 2a). In Fig. 4b the welded specimens are showed, whilst in Table 1 the optimized welding parameters ranges are described.

3. Mechanical characterization of the CD welded bars

3.1. Tensile and creep tests

Tensile and creep tests have been executed onto base metal and as-welded specimens with the same heat treatments described in Table 2, at room and operating temperatures (650 °C and 400 °C for Inconel 718 and Ti alloy, respectively). The performed heat treatments have been selected to remove residual stresses after welding and redistribute the precipitates in the less severe manner, using low

Table 2
Post-welding heat treatments

Material	HT type	HT details
Inconel 718	Solution + precipitation	Vacuum 955 °C for 1 h + 720 °C for 8 h + 620 °C for 8 h; gas fan quenching
Ti alloy – 1° HT type	Stress relieving only	Vacuum 600 °C for 1 h minimum; gas fan quenching
Ti alloy – 2° HT type	Annealing + solution	Vacuum 950 °C for 1 h in argon; ventilated quenching

temperature levels and retaining the subsequent undesirable thermal deformations (for repair purposes these deformations are to be avoided); the Ti alloy specimens have been treated in two different ways, in order to improve the mechanical weld characteristics.

All the mechanical tests specimens have been machined with the same geometry, according to the standard codes. The creep and fatigue specimens have also been accurately polished to reach 0.4 R_a roughness; particular care has been taken to respect axiality and fillet radius values.

Tables 3–5 show the tensile and creep rupture tests results of the welded specimens, two and three tests for each condition. V_t is the loading rate and E the Young modulus, measured according to the actual recommendations and with the use of HT elongation transducers; the yield stress R_p, and the ultimate tensile stress R_m have been normalised with respect to the base material properties σ_y and σ_u, measured on the first four bars of identical geometry and HT conditions for both the materials; particular care has been used to avoid drift and offset errors.

Table 3
Tensile test data for Inconel 718 specimens

Inc 718	Welded specimens				
Specimen No.	I5	I6	I7	I8	I9
T (°C)	25	25	650	650	650
V_t (mm/min)	0.075	0.075	0.040	0.040	0.040
E (N/mm^2)	201170	195300	184650	223990	175350
R_p 0.2%/σ_y	1.021	1.029	0.973	0.795	0.978
R_m/σ_u	0.841	0.875	0.807	0.659	0.894

According to the obtained results, the tensile tests show good static behaviour of the Inconel 718 CDW welded joints, Fig. 5a, particularly in terms of yield stresses at room and working temperature (the proof strength is slightly below the minimum base material specifications at elevated temperature, as stated in Table 3). On the other hand, the Ti alloy welded specimens with the first heat treatment seem to offer poor tensile properties (Table 4); the yield stresses and ultimate stresses are 20–30% lower than the base material. In Fig. 5b the traction curves for the TiAl6V4 alloy jointed bars are reported. The same specimens exhibit considerably higher tensile properties if the second and more severe heat treatment is used; thereafter the specimens for the fatigue tests have also been solu-

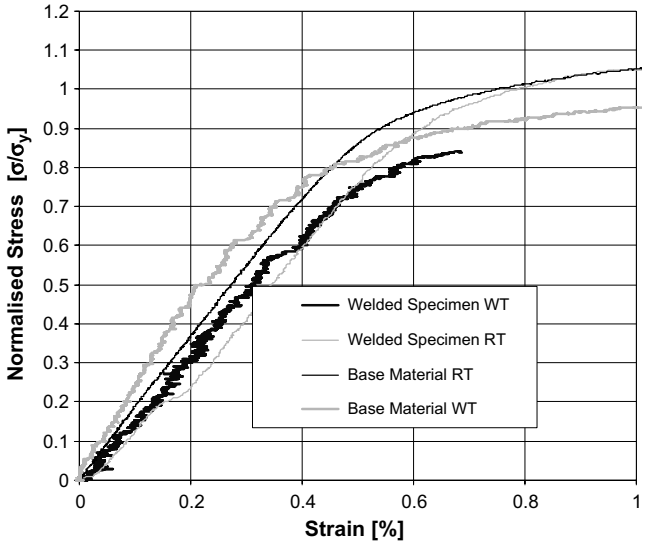

Fig. 5a. Inc 718 Welded material tensile behaviour.

Table 4
Tensile test data for Ti alloy specimens

Ti alloy	Welded specimens (HT 1)					Welded specimens (HT 2)			
Specimen No.	T5	T6	T7	T8	T9	T10	T11	T12	T13
T (°C)	25	25	400	400	400	25	25	400	400
V_t (mm/min)	0.120	0.120	0.075	0.075	0.075	0.120	0.120	0.075	0.075
E (N/mm^2)	105220	105780	94560	86833	88044	n.a.	n.a.	n.a.	n.a.
R_p 0.2%/σ_y	0.874	0.769	0.974	0.564	0.686	1.001	1.002	0.983	0.968
R_m/σ_u	0.799	0.703	0.822	0.475	5.875	0.992	1.003	0.976	1.004

Table 5
Creep tests results (as-welded specimens normalised with respect to base materials)

Specimen No.	1	2	3	4	5	6	7	8	9	10
Material	Inc 718	Inc 718	Ti6Al4V4	Ti6Al4V4	Inc 718	Inc 718	Inc 718	Ti6Al4V4	Ti6Al4V4	Ti6Al4V4
Condition	Base mat.	Base mat.	Base mat.	Base mat.	Welded	Welded	Welded	Welded	Welded	Welded
Temperature (°C)	650	650	400	400	650	650	650	400	400	400
Load: $\sigma_{welded}/\sigma_{base\ mat.}$	1.00	1.00	1.00	1.00	0.73	0.43	0.58	0.41	0.50	0.62
Rupture time (h)	82	216	536	920	1	38	13	1008	720	0.5

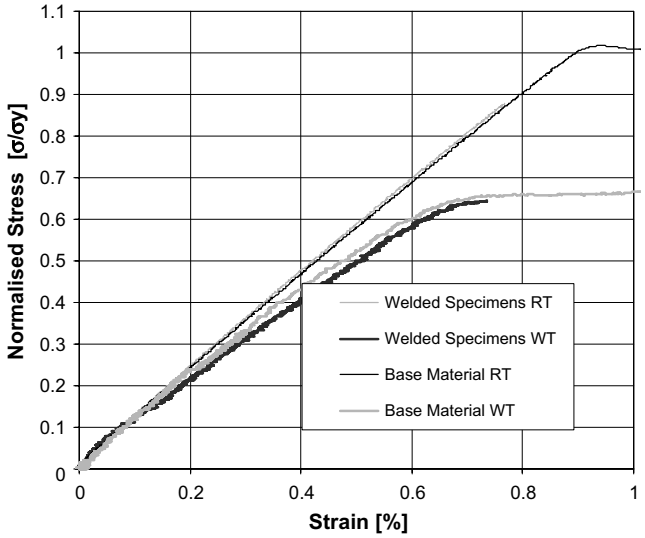

Fig. 5b. TiAl6V4 Welded material tensile behaviour.

tion-annealed. In Figs. 5a and 5b are reported the traction behaviour with the curves achieved from tensile tests for both welded materials with respect to the base metal at room and working temperature.

All the welded bars exhibit very low elongation percentages ($A = 0.5$–2%, not reported in tables) according to the fact the tensile direction is orthogonal to the thin welded profile; consequently all the tensile tests show the yield stress at the same level of the ultimate stresses as showed in Figs. 5a and 5b. The plastic collapse of the welded metal is retained in very small regions of the specimens while the base material is kept in elastic conditions.

Concerning the Inconel 718 base material in the heat treatment conditions of annealing and aging at intermediate temperatures, the tensile strength at room and working temperature is higher than the minimum prescribed values by the Aerospace Structural Metals Handbook, 1972 (minimum 1275 N/mm^2) [17]. Therefore the welded material at room temperature presents a tensile strength slightly lower than the ASM reference strength. This fact takes into account the CDW welded bars are very different among themselves as showed in Tables 3 and 4, depending on the weld cord irregularities.

The TiAl6V4 specimens have been tested in two different post-welding heat treatment conditions: the first heat treatment is less severe than the ASM prescribed one; the second treatment is more severe and differs from the conventional treatments. In the first case, at room temperature the Ti alloy base material tensile strength is lower than the minimum prescribed by the ASM (1104 N/mm^2), while at the temperature of 400 °C, the tensile strength is higher. On the other hand, the welded material at room temperature presents a tensile strength lower than the base material reference values (Table 3), and the difference increases at the temperature of 400 °C. In the second heat treatment conditions, the values for the base material are slightly lower, at room temperature and high temperature; on the contrary, the welded specimens present higher tensile and yield strength with respect to the base material results with identical post-welding heat treatments, at room and high temperature.

In Fig. 6, the typical creep-stress rupture curves for the base materials are represented and agree with the technical literature data [15,16]. The reference temperatures are 650 °C for Inc 718 and 400 °C for TiAl6V4 alloy and the selected stresses are chosen to produce rapid creep deformations and failure. The CD welded specimens with the multipoint technique have been tested under creep at the same conditions with specimens of 6.25 mm diameter; the results are reported in Table 5. Being the creep rupture times extremely short for the welded specimens, the applied stresses have been reduced with respect to the base metal. While the endurance is equal to 200 h for the Inc 718 base material, in the welding conditions at the same load and temperature, the failure is instantaneous. This occurs also for the Ti alloy welded specimens and if the load is nearly halved. Only with loads 45% lower than the base material, the Inc 718 welded specimen No. 6 reaches creep endurances in the order of 40 h.

At temperature of 400 °C and lower loads (around 40% the base material reference stress), the Ti welded specimens endurance is over 700 h; if the load increases 20% more, the endurance decreases brusquely and when the load decreases of 25%, the endurance increases significantly. This reveals the CD welds are extremely brittle also under

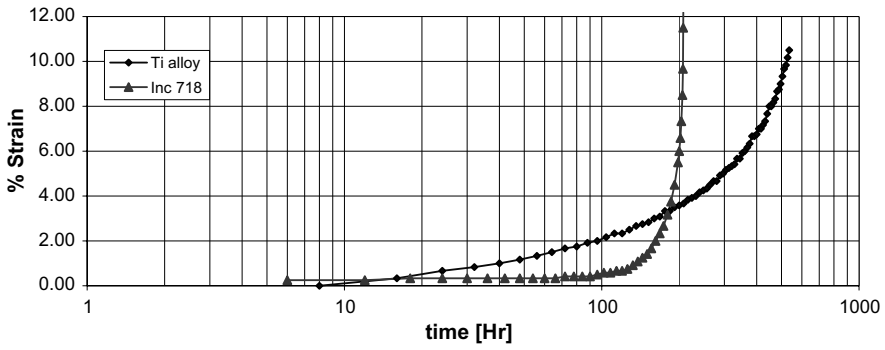

Fig. 6. Base material creep test results. Specimens 2 and 3.

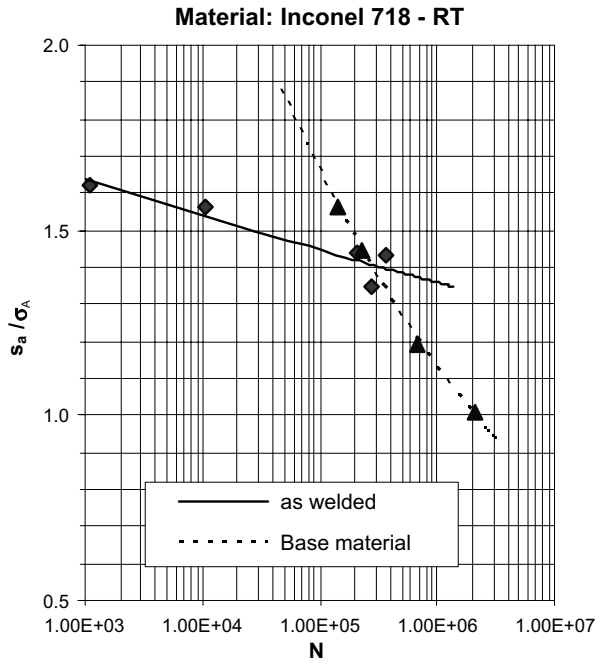

Fig. 7a. Fatigue tests of Inconel 718 at room temperature.

long lasting loads at elevated temperatures and the deformations seem excessively reduced with respect to the base material; the creep behaviour is strongly affected by the weld presence and the microstructure has to be investigated or the process is to be modified in order to improve the elongation characteristics of the welded layer. All the specimens have been heat treated according to Table 2 data (for the Ti specimens, the first HT has been used).

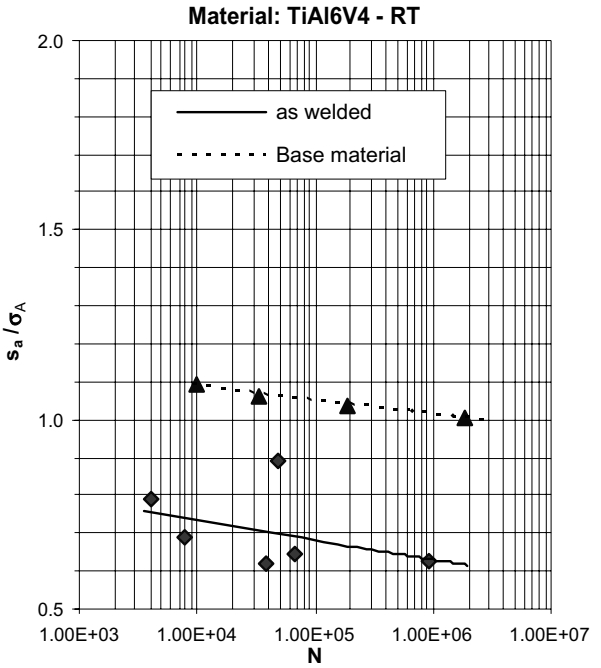

Fig. 7b. Fatigue tests of TiAl6V4 at room temperature.

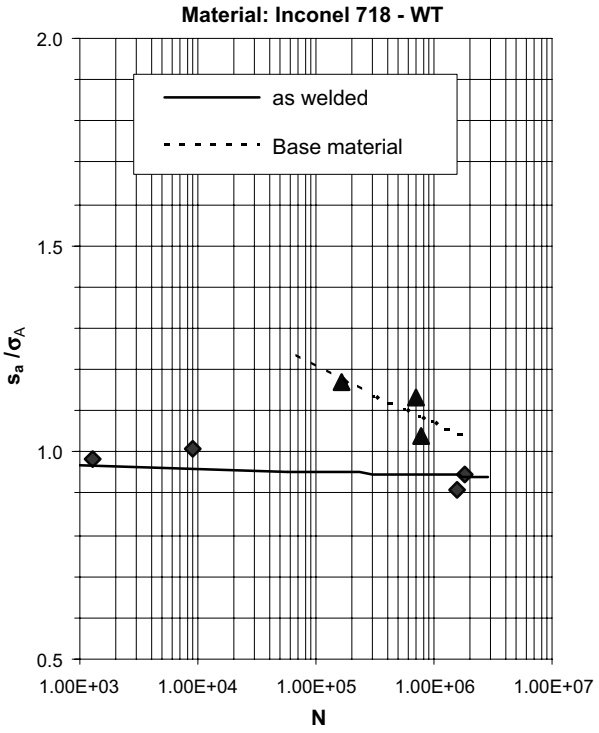

Fig. 8a. Fatigue tests of Inconel 718 at high temperature.

3.2. Fatigue tests

The fatigue Wöhler curves achieved for both the materials are presented in Figs. 7 and 8, normalised with respect to the base material limit stresses at 2×10^6 cycles. The tests have been conducted with standard specimens of 6.00 mm

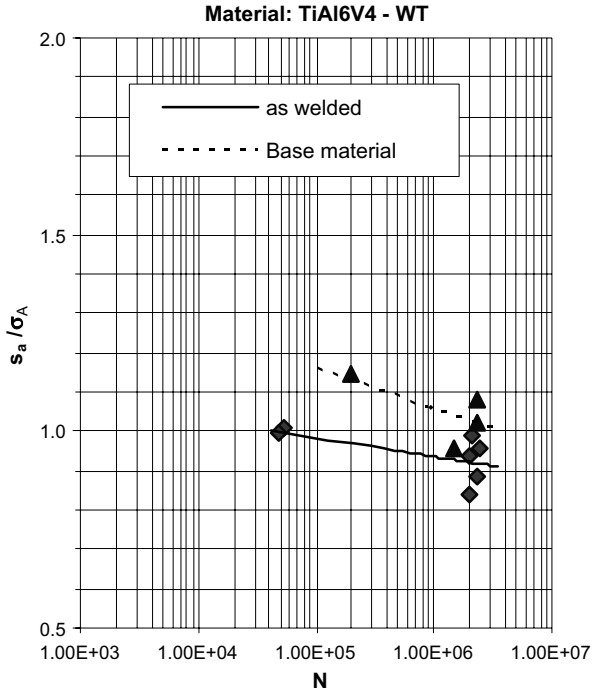

Fig. 8b. Fatigue tests of TiAl6V4 at high temperature.

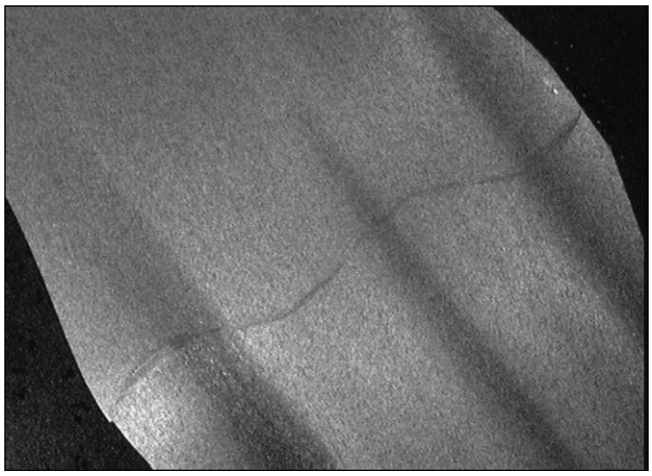

Fig. 9a. Longitudinal joint section and distribution of the welded metal profile. Ti alloy.

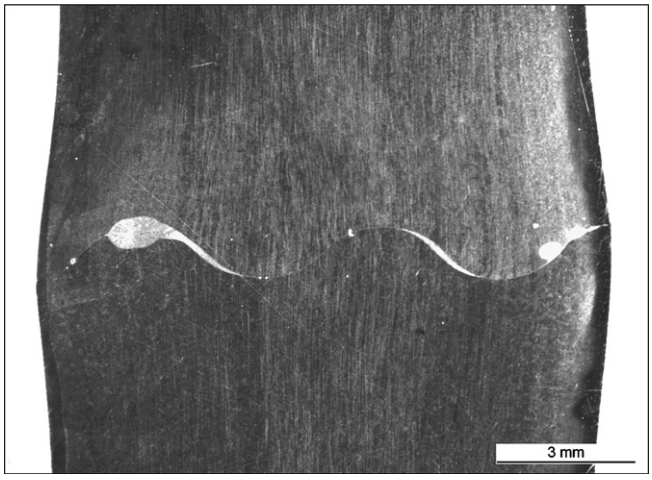

Fig. 9b. Longitudinal joint section and distribution of the welded metal profile. Inconel 718.

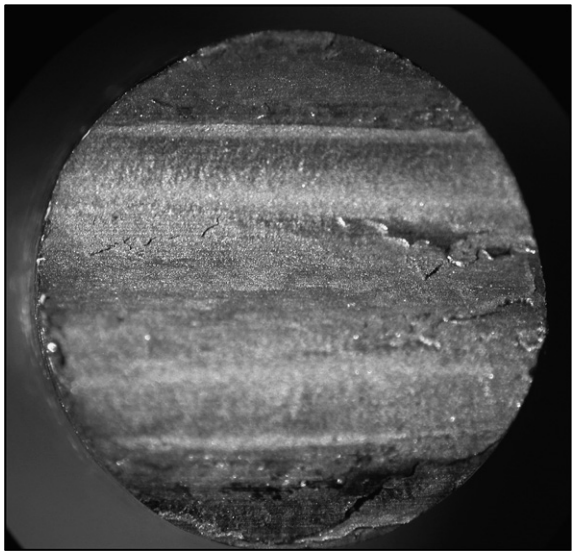

Fig. 10a. Tensile rupture surfaces. Inconel 718.

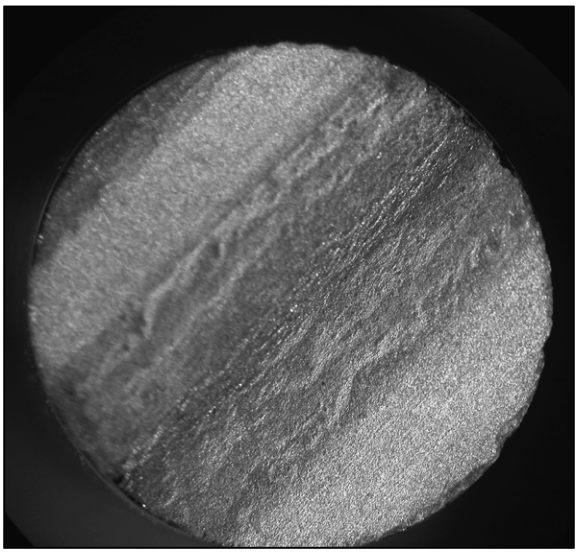

Fig. 10b. Tensile rupture surfaces. TiAl6V4.

diameter and with $R = \sigma_{min}/\sigma_{max} = 1$ at room temperature and high temperature (650 °C for Inconel 718 and 400 °C for Ti alloy specimens). All the specimens have been heat treated together with the tensile and creep specimens; in particular, the TiAl6V4 welded specimens have been heat treated with the second HT in Table 2, since this resulted in better mechanical behaviour for the Ti welded bars. The general results are coherent with the static results; the fatigue curves are displayed in Figs. 7a, 7b, 8a, 8b; the welded specimens show lower dynamic resistance capabilities with respect to the base materials.

Despite the small number of specimens, some curves indications can be clearly observed. The base material trend is in good agreement with literature data [11–14] and with the static tests results either at room and high temperature, while the flat-slope trend of the welded specimen data is strongly dependent on the CD weld material microstructure and characteristics, which lead Wöhler points to be settled in a narrow band in terms of stress amplitude. It appears in fact, the fatigue endurance for

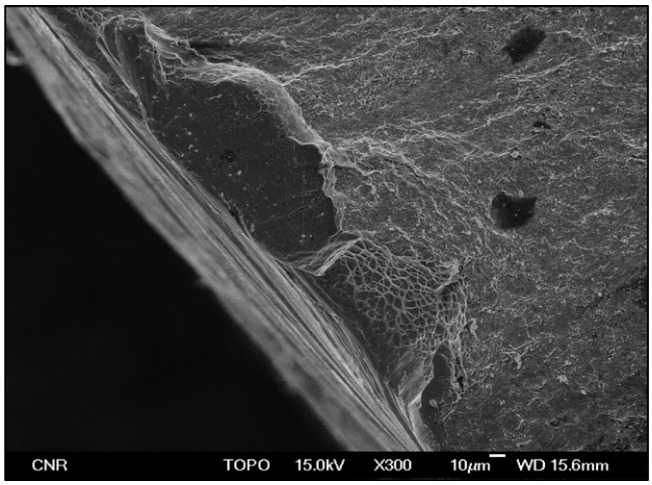

Fig. 10c. Probable rupture initiation of Ti welded surface with SEM.

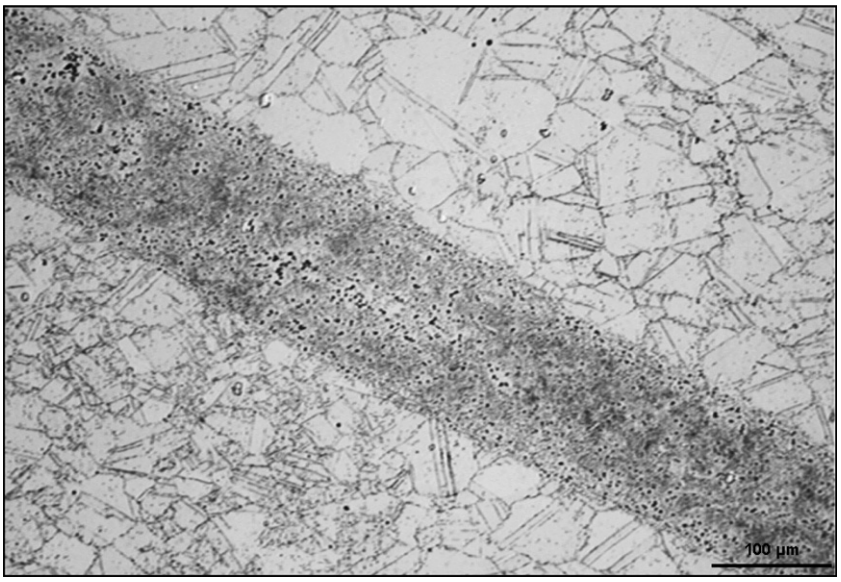

Fig. 11. Inconel 718 average welded profile aspect.

both the welded materials to drop suddenly below a certain load level, easily expresses in the diagrams as function of the ratio σ_a/σ_A with respect to the base material. The curves are mutually positioned one respect the other with a specific reduction factor, calculated roughly as average of the stress amplitude differences (a reduction factor of 0.8 for the Inconel 718 welded joints and equal to 0.7 for the titanium welded joints at room temperature; values of 0.9 for Inconel 718 and 0.8 for titanium at high temperature), probably due to the brittle character of the welded joints and to the nearly absent HAZ; above these limits the CD welded specimens exhibit good endurance properties reaching often fatigue lives over millions of cycles. It is certainly possible to indicatively estimate these limit values as the "fatigue limits" of the welded bars if the base material fatigue limits are assessed.

At operational temperatures the results show a similar behaviour, but the stress limit values are stabilized to higher levels proportionally to the respective static proof stresses, resulting in encouraging fatigue properties for this type of welded joints applied to aeronautical materials (the stress amplitudes above 10^6 cycles are slightly lower than the base material amplitudes for Ti alloy and especially the Inconel 718 superalloy, as displayed in Figs. 8a and 8b).

The static and fatigue strength of the CD Welded circular bars is proved to be acceptable for both the materials,

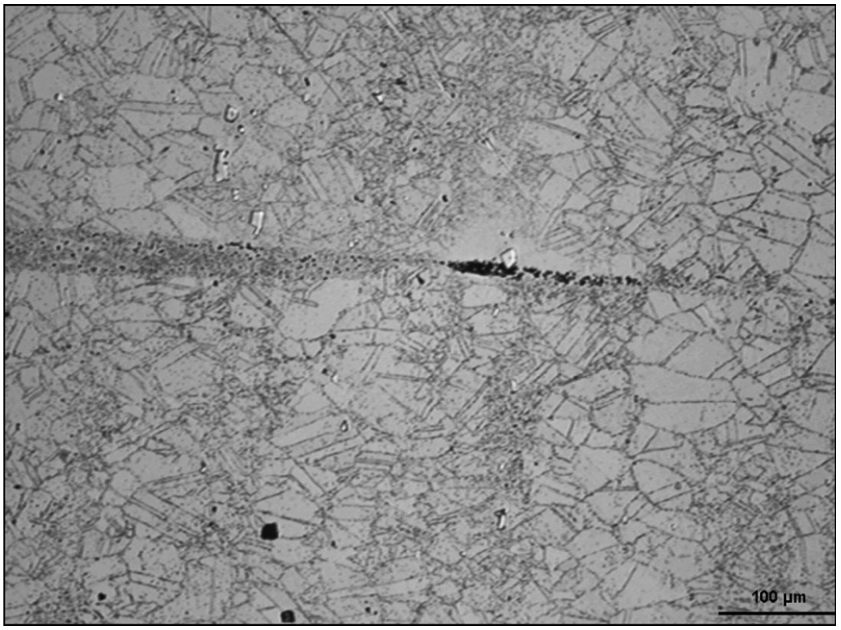

Fig. 12. Inconel 718 welded profile discontinuity.

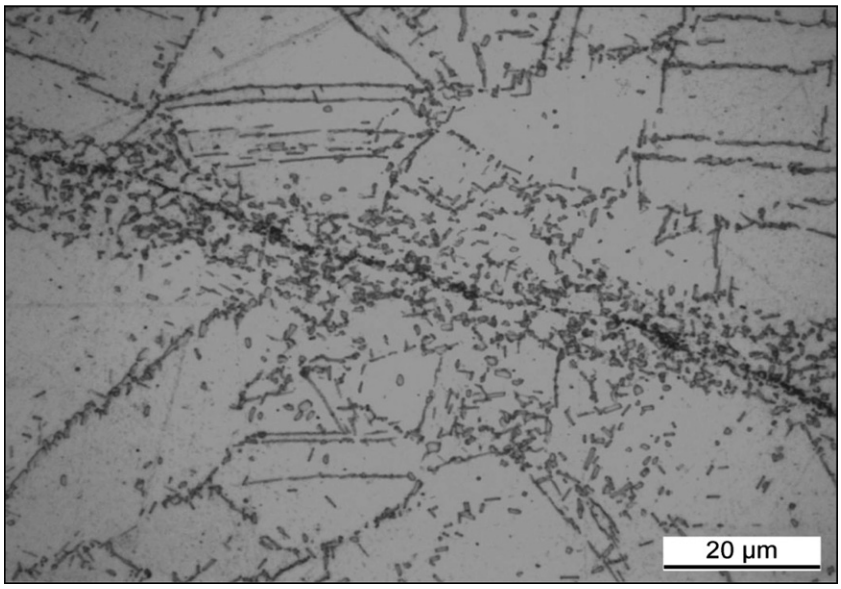

Fig. 13. Inconel 718 thinner welded layer zone.

considering several improvements can still be done in terms of welding parameters changes, heat treatments selections and multicontact profile modifications.

4. Microstructure of CDW welded aeronautical alloys

In Figs. 9a and 9b, the longitudinal welded section of both materials is displayed; the welded layer is extremely thin (in the order of 0.05–0.3 mm), with discontinuous thickness along the multipoint profile. Fusion is achieved all over the welded surface to be jointed for the Ti alloy welds, but in the case of Inc 718, the sparsely thin transition zones at the contact peaks indicate near-to-bonding weld characteristics. No pores or evident microcracks are to be observed. The failure surface after tensile tests follows in all cases the welding profile and appears very smooth and regular; in Figs. 10a, 10b and 10c asperities are not observed and cleavage fracture is recognizable; ductility is apparently not present since the deformations are limited in small layers of the welded metal. The welded metal distribution appears well deposed all over the weld line in extremely thin layers of variable thickness as in Fig. 11 for both materials; although not uniform molten metal deposition can be observed in Figs. 12 and 15 and microdefects presence is detected in the form of small vain localized at the transition point between the peak zones and the

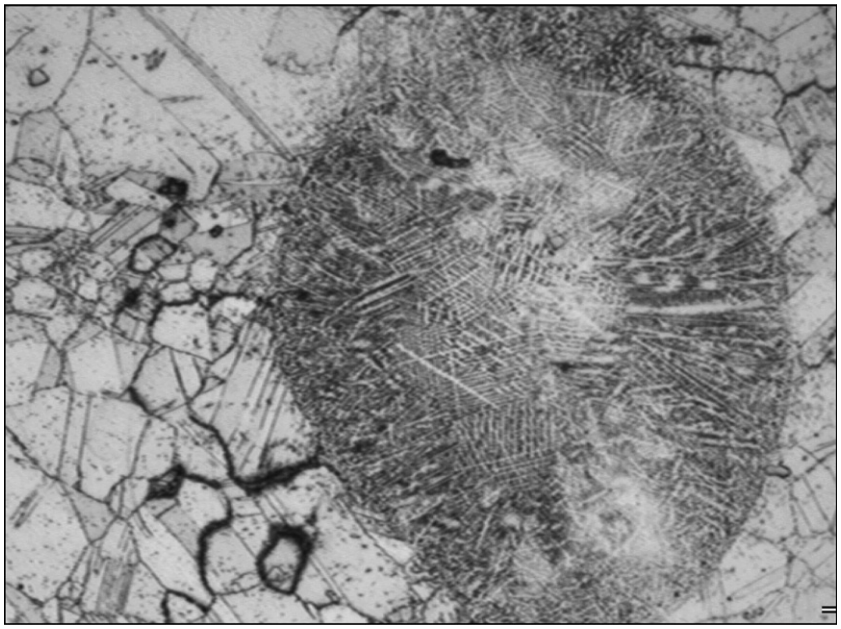

Fig. 14. Inc 718 hot spot and defects in the borders.

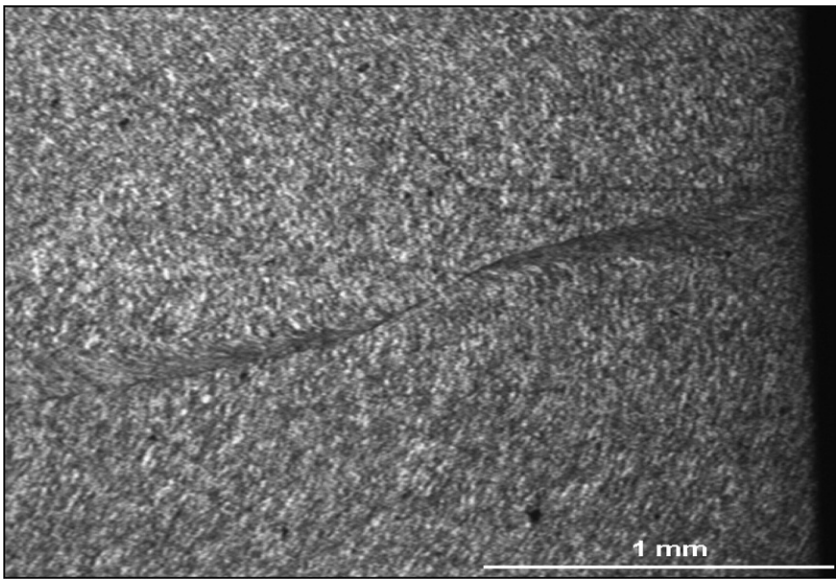

Fig. 15. Ti deformed microstructure CD Welding.

gaps filled with fused metal. The welded layer appears sufficiently coherent with the base materials (Figs. 13 and 16); in the case of Inconel 718 specimens, the microstructure is characterized by stratified precipitates along the weld border and very fine granulometry with small grain dimension (Figs. 13 and 14) also in the thinner weld zone. Similar considerations can be arisen for the Ti-alloy welded specimens in Figs. 17 and 18, but larger deformations occur in the microstructure, leading to visible new grain orientation perpendicular to the weld. The rupture mechanism is equally recognizable as brittle fracture on the whole surface, but small plastic deformation is sparsely observed in restricted zones (Figs. 10a and 10b) where the thin welded metal layer is stretched between the substrates of base material and keeps stuck alternatively to one of the two boundaries giving rise to plastic transition sites. The probable point of initiation of rupture is localized at the weld borders as indicated by Fig. 10c. In Figs. 9 and 14, it is clearly observed the hot spot located at the border regions in the Inc 718 welded bars. This zones microstructure is strongly modified and large precipitate density within the dendrite resolidified material spot; this phenomenon is originated by electro-magnetic interactions with the material dielectrical properties during the welding discharge. This effect, together with the presence of discontinuities welded zones as in Fig. 12, are to be eliminated with different welding parameters choice or decreasing the local power input, in order to elevate the mechanical strength.

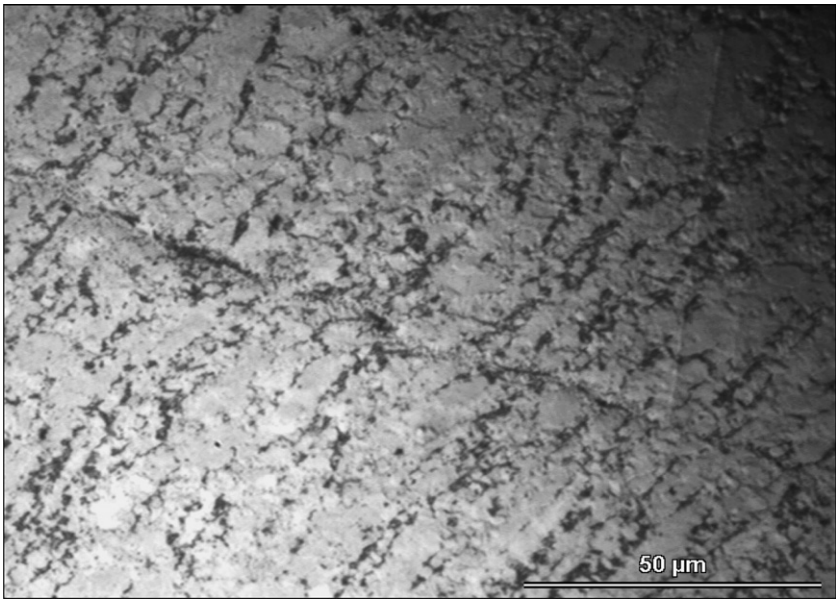

Fig. 16. Detail of the weld interface with base metal.

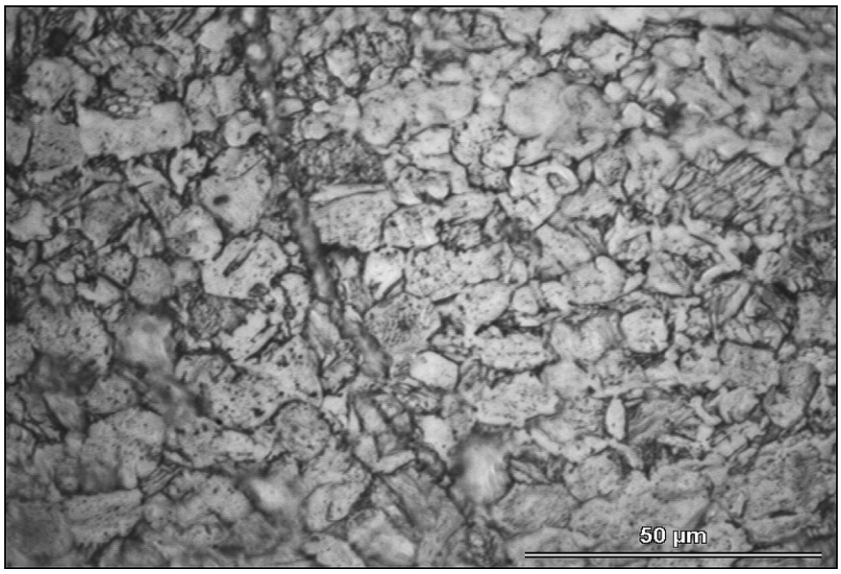

Fig. 17. Stratified precipitates in the Ti CD Welded layer.

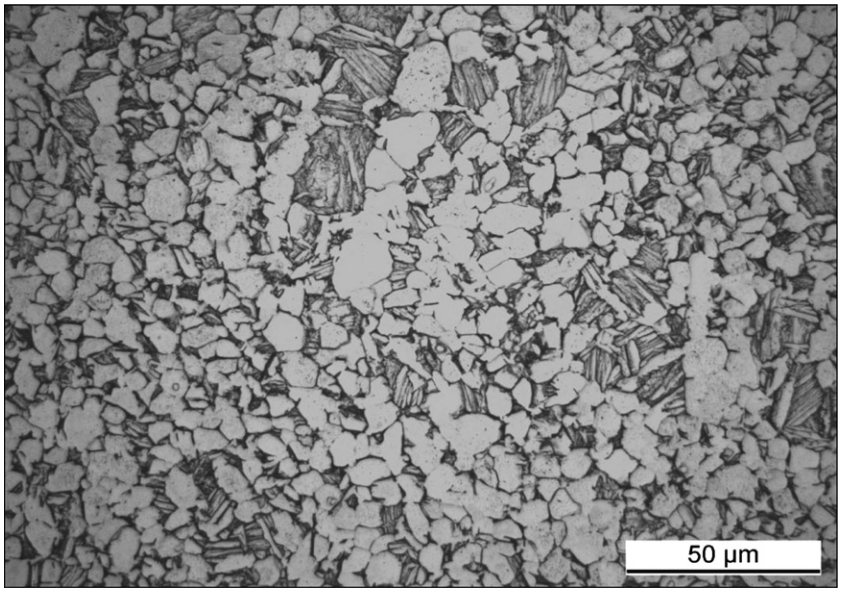

Fig. 18. Grain orientation beside the joined area.

5. Conclusions

This paper shows the CDW process with the multipoint procedure can be employed for repair and production of complex parts in aeronautical materials; in fact encouraging results in terms of tensile and creep strength for future applications have been achieved, despite the fact a brittle character of the welded joints has been encountered because of the observed cleavage rupture mode of the samples; nevertheless the fatigue tests on welded specimens exhibit sufficiently good life endurances with respect to the base metal if the needed heat treatments are used.

However, in order to operatively employ the technology in the production industry and to validate its potential and strategic role, the principal parameters (applied force and energy, discharge time and maximum discharged current) can still be optimized, and the welding tools for the processing technology can be improved through pre-heating procedures and multiple discharges of the pieces before welding. The microstructural study allowed to detect the initiation points of small defects along the profiled welded layers; these defects can be eliminated through different multipoint contact geometries and higher and uniform heat input throughout the welded section.

References

[1] Dattoma V, Panella FW. Studio della Resistenza su Saldature CDW di barre in acciaio AISI 304. XXXII Convegno AIAS, Salerno–Italy; 2003.

[2] Casalino G, Dattoma V, Ludovico A, Panella FW. Numerical model for capacitor discharge welding. 13th DAAAM international symposium, Vienna–Austria; 2000.
[3] Chiozzi S, Dattoma V, Panella FW. First results on the mechanical behaviour of CDW welded superalloys. 5th International conference on fatigue and fracture, Bari, Italy; 2005.
[4] Venkataraman S, Devlietan JH. Rapid solidification of stainless steels by capacitor discharge welding. Weld Res Supplement to the Weld J 1988.
[5] Wilson RD. Explore the potential of capacitor discharge welding. Adv Mater Process 1994;145(6):93–4.
[6] Kristiansen M. Pulsed power applications. Conf Proc JIEE- IPEC'95, Yokohama–Japan, pp. 1391–6.
[7] Alley RL. Capacitor discharge study welding. ASM handbook, welding, brazing and soldering, vol. 6. American Welding Society; 1991.
[8] Dattoma V, Nobile R, Panella FW, Tafuro R. Analisi FEM termomeccanica del processo di saldatura a scarica capacitiva di tipo multipoint. Conf Proc XXXIII Convegno AIAS, Bari–Italy; 2004.
[9] Wilson RD, Woodyard JR, Devletian JH. Capacitor discharge welding: analysis through ultrahigh speed photography. Weld Res Supplement to the Weld J 1993.
[10] Matsugi K, Wang Y, Hatayama T, Yanagisawa O, Syakagohre K. Application of electric discharge process in joining aluminium and stainless steel sheets. J Mater Process Technol 2003;135: 75–82.
[11] Sims CT. Superalloys. In: Gell M et al., editors, The Metallurgical Society of AIME: Warrendale; 1984. p. 399.
[12] Serin K, Neuser RD, Eggeler G, Kamaraj M, Kolbe M, Heitkemper M. Prakt Metallogr 2001;38:679.
[13] Matsugi K, Konishi M, Yanagisawa O, Kiritani M. Joining of spheroidal graphite cast iron to stainless steel by impact-electric current discharge joining. J Mater Process Technol 2004;150: 300–8.
[14] Sundaresan S, Janaki Ram GD, Madhusudhan R. Microstructural refinement of weld fusion zones in a-b titanium alloys using pulsed current welding. Mater Sci Eng 1999;A262:88–100.
[15] Serin K, Eggeler G. In: Parker JD, editor. Creep and fracture of engineering materials and structures. London: The Institute of Materials; 2001. p. 385.
[16] Constant amplitude axial Fatigue tests on metallic materials. ASTM Standards E 466-72 T – US.
[17] ASM Handbook. Battelle-Columbus Laboratories, Ohio, US; 1972.